Clim. Past, 13, 1451–1471, 2017
https://doi.org/10.5194/cp-13-1451-2017

Climate of the Past
Open Access
EGU

Climate signals in a multispecies tree-ring network from central and southern Italy and reconstruction of the late summer temperatures since the early 1700s

Giovanni Leonelli[1], Anna Coppola[2], Maria Cristina Salvatore[2], Carlo Baroni[2,3], Giovanna Battipaglia[4,5], Tiziana Gentilesca[6], Francesco Ripullone[6], Marco Borghetti[6], Emanuele Conte[7], Roberto Tognetti[8], Marco Marchetti[7], Fabio Lombardi[9], Michele Brunetti[10], Maurizio Maugeri[10,11], Manuela Pelfini[12], Paolo Cherubini[13], Antonello Provenzale[3], and Valter Maggi[1,3]

[1]Dept. of Earth and Environmental Science, Università degli Studi di Milano–Bicocca, Milan, Italy
[2]Dept. of Earth Sciences, Università degli Studi di Pisa, Pisa, Italy
[3]Istituto di Geoscienze e Georisorse, Consiglio Nazionale delle Ricerche, Pisa, Italy
[4]Dept. DiSTABiF, Università degli Studi della Campania "L. Vanvitelli", Caserta, Italy
[5]PALECO EPHE, University of Montpellier 2, Montpellier, France
[6]School of Agricultural, Forestry, Food and Environmental Sciences, Università degli Studi della Basilicata, Potenza, Italy
[7]Dept. of Biosciences and Territory, Università degli Studi del Molise, Campobasso, Italy
[8]Dept. of Agricultural, Environmental and Food Sciences, Università degli Studi del Molise, Campobasso, Italy
[9]Dept. of Agronomy, Università Mediterranea di Reggio Calabria, Reggio Calabria, Italy
[10]Istituto di Scienze dell'Atmosfera e del Clima, Consiglio Nazionale delle Ricerche, Bologna, Italy
[11]Dept. of Environmental Science and Policy, Università degli Studi di Milano, Milan, Italy
[12]Dept. of Earth Sciences, Università degli Studi di Milano, Milan, Italy
[13]Swiss Federal Institute for Forest, Snow and Landscape Research WSL, Birmensdorf, Switzerland

Correspondence to: Giovanni Leonelli (giovanni.leonelli@unimib.it)

Received: 14 March 2017 – Discussion started: 17 March 2017
Revised: 25 August 2017 – Accepted: 16 September 2017 – Published: 2 November 2017

Abstract. A first assessment of the main climatic drivers that modulate the tree-ring width (RW) and maximum latewood density (MXD) along the Italian Peninsula and northeastern Sicily was performed using 27 forest sites, which include conifers (RW and MXD) and broadleaves (only RW). Tree-ring data were compared using the correlation analysis of the monthly and seasonal variables of temperature, precipitation and standardized precipitation index (SPI, used to characterize meteorological droughts) against each species-specific site chronology and against the highly sensitive to climate (HSTC) chronologies (based on selected indexed individual series). We find that climate signals in conifer MXD are stronger and more stable over time than those in conifer and broadleaf RW. In particular, conifer MXD variability is directly influenced by the late summer (August, September) temperature and is inversely influenced by the summer precipitation and droughts (SPI at a timescale of 3 months). The MXD sensitivity to August–September (AS) temperature and to summer drought is mainly driven by the latitudinal gradient of summer precipitation amounts, with sites in the northern Apennines showing stronger climate signals than sites in the south. Conifer RW is influenced by the temperature and drought of the previous summer, whereas broadleaf RW is more influenced by summer precipitation and drought of the current growing season. The reconstruction of the late summer temperatures for the Italian Peninsula for the past 300 years, based on the HSTC chronology of conifer MXD, shows a stable model performance that underlines periods of climatic cooling (and likely also wetter conditions) in 1699, 1740, 1814, 1914 and 1938, and follows well the variability of the instrumental record and of other tree-ring-based reconstructions in the region. Considering a

20-year low-pass-filtered series, the reconstructed temperature record consistently deviates < 1 °C from the instrumental record. This divergence may also be due to the precipitation patterns and drought stresses that influence the tree-ring MXD at our study sites. The reconstructed late summer temperature variability is also linked to summer drought conditions and it is valid for the west–east oriented region including Sardinia, Sicily, the Italian Peninsula and the western Balkan area along the Adriatic coast.

1 Introduction

Climate reconstructions for periods before instrumental records rely on proxy data from natural archives and on the ability to date them. Among the available proxies, tree rings are one of the most used archives for reconstructing past climates with annual resolution in continental areas and they often come from the temperature-limited environments with high latitudes and altitudes (e.g., Briffa et al., 2004; Rutherford et al., 2005). Tree-ring data can be used at regional to global scales (IPCC, 2013) and long chronologies covering millennia, going back as far as the early Holocene, are available (for Europe: Becker, 1993; Friedrich et al., 2004; Nicolussi et al., 2009).

The reconstruction of past climate variability and the analysis of its effects on forest ecosystems are crucial elements for understanding climatic processes and for predicting what responses should be expected in ecosystems under the ongoing climatic and global changes. In particular, the Mediterranean region is a prominent climate change hot spot (Giorgi, 2006; Turco et al., 2015), and by the end of this century, it will likely experience a regional warming higher than the global mean (up to +5 °C in summer) and a reduction of the average summer precipitation (up to −30 %; Somot et al., 2007; IPCC, 2013). As a consequence of the poleward expansion of the subtropical dry zones (e.g., Fu et al., 2006), subtropical environments under climate change are already facing strong hydroclimatic changes due to lower precipitation and human exploitation (e.g., in southwestern North America; Seager et al., 2007; Seager and Vecchi, 2010). Moreover, in these environments (including the Mediterranean region), soil moisture will likely drop, resulting in a contraction of temperate drylands by approximately a third (converting into subtropical drylands), and longer periods of drought in deep soil layers are expected (Schlaepfer et al., 2017). The increase in drought conditions during the growing season is already negatively impacting tree growth, especially at xeric sites in the southwestern and eastern Mediterranean (e.g., Galván et al., 2014). At the ecosystem level, in the near future, the responses to climate changes will impact the various forest species in a different way, depending on their physiological ability to acclimate and adapt to the new environmental conditions (e.g., Battipaglia et al., 2009; Ripullone et al., 2009), and on their capacity to grow, accumulate biomass and contribute as sinks in the terrestrial carbon cycle. Natural summer fires in the Mediterranean area are also expected to increase in frequency over the coming decades as a response to increasingly frequent drought conditions, assuming a lack of additional fire management and prevention measures (Turco et al., 2017).

1.1 Tree-ring response to climate

Climate–growth relationships have been studied for several species in the Mediterranean region, with different objectives: forest productivity (e.g., Biondi, 1999; Boisvenue and Running, 2006; Nicault et al., 2008; Piovesan et al., 2008; Babst et al., 2013), tree ecophysiology, wood formation and related dating issues (Cherubini et al., 2003; Battipaglia et al., 2014), sustainability of forest management (e.g., Boydak and Dogru, 1997; Barbati et al., 2007; Marchetti et al., 2010; Castagneri et al., 2014), provision of ecosystem services (e.g., Schröter et al., 2005) such as carbon sequestration (e.g., Scarascia-Mugnozza and Matteucci, 2014; Calfapietra et al., 2015; Borghetti et al., 2017), effective biodiversity conservation (e.g., Todaro et al., 2007; Battipaglia et al., 2009) and climate reconstruction (see next section), which have led to a variety of associations between climate variables and growth responses in conifers and broadleaves from different environments and ecosystems. Mainly considering the species of this study, we report the main findings on the climate–growth responses found in this region.

Conifers. Studies on silver fir (*Abies alba* Mill.) growth in the Italian Peninsula reveal high sensitivity to the climate of the previous summer, August$_{-1}$ in particular, and show positive correlations with precipitation and negative correlations with temperature (Carrer et al., 2010; Rita et al., 2014). Moreover, tree growth in this region is moderately negatively correlated with the temperature of the current summer (unlike that in stands located in the European Alps; Carrer et al., 2010), namely, high temperatures in July and August negatively affect tree growth. A dendroclimatic network of pines (*Pinus nigra* J. F. Arnold and *P. sylvestris* L.) in east-central Spain shows that drought (namely, the standardized precipitation–evapotranspiration index – SPEI; Vicente-Serrano et al., 2010) is the main climatic driver of tree-ring growth (Martin-Benito et al., 2013). In a *P. uncinata* network from the Pyrenees, an increasing influence of summer droughts (SPEI) on tree-ring widths (RW) during the 20th century as well as the control of May temperatures on maximum latewood density (MXD) is found (Galván et al., 2015). However, in the abovementioned analyses, the possible influences of the summer climate variables from the year prior to the growth were not considered. Elevation, and particularly the related moisture regime, in the eastern Mediterranean region is the main driver of tree-ring growth patterns in a multispecies conifer network comprised of *P. nigra*, *P. sylvestris* and *P. pinea* L. specimens (Touchan et al., 2016). A dipole pattern in tree-ring growth variability is reported

for Mediterranean pines ranging from Spain to Turkey, with higher sensitivity to summer drought in the east than in the west, and with higher sensitivity to early summer temperature in the west (Seim et al., 2015). Strong correlations between autumn-to-summer precipitation and tree-ring growth and between summer drought and tree-ring growth have been reported for sites (mainly of conifers) in northern Africa–western Mediterranean, with trees in Morocco also responding to the North Atlantic Oscillation index (Touchan et al., 2017).

Broadleaves. In the western Mediterranean (northern Morocco, Algeria, Tunisia, Italy and southern France), deciduous oaks, including *Quercus robur* L., reveal a direct response of tree-ring growth to summer precipitation and an inverse response to summer temperature (Tessier et al., 1994). Beech (*Fagus sylvatica* L.) is particularly sensitive to soil moisture and air humidity; in past decades, long-term drought conditions have been shown to be the main factor causing a growth decline in the old-growth stands in the Apennines (Piovesan et al., 2008). Beech shows different responses to climate at high- vs. low-altitude sites (Piovesan et al., 2005), with the latter being positively affected by high May temperatures. Despite an expected higher drought sensitivity stress close to the southern limit of the distribution area, a late 20th century tree-ring growth increase in beech has been reported in Albania (Tegel et al., 2014), thus underlining the different climate–growth responses in the Mediterranean region. Beech, indeed, presents complex climate growth-responses and also appears to be a less responsive species in the Mediterranean area when compared to conifers such as *P. sylvestris, P. nigra, P. uncinata* or *A. alba* (as found in southeastern France; Lebourgeois et al., 2012).

1.2 Tree-ring-based climate reconstructions

One of the most powerful tools in terrestrial paleoclimatology is obtaining date information about the past climate and past environmental conditions in a region by analyzing the tree rings. However, in the Mediterranean region, the low temporal stability of the recorded climatic signals (e.g., Lebourgeois et al., 2012; Castagneri et al., 2014), the scarcity of long chronologies and the high variability of climatic and ecological conditions (Cherubini et al., 2003) often make this analysis difficult. Ring widths are among the most used variables for climate reconstruction but they usually show higher temporal instability in their relationship with climate than that of maximum latewood density (for the Pyrenees, see Büntgen et al., 2010).

The potential to analyze relatively long chronologies in the Mediterranean region has allowed for the reconstruction of the past climate (mainly precipitation and droughts). Several reconstructions of May–June precipitation have been performed, mainly over the last 300–400 years, in a region including northern Greece, Turkey and Georgia: in northern Aegean–northern Anatolia a tree-ring network of oaks was used for reconstructing precipitation variability from 1089 (Griggs et al., 2007); in the Anatolian Peninsula a mixed conifer–broadleaf tree-ring network (mainly *P. nigra*, *P. sylvestris* and oaks; Akkemik et al., 2008), a *P. nigra* network (Köse et al., 2011) and a multi-species conifer network (mainly *P. nigra*, *P. sylvestris* and *Abies nordmanniana* (Steven) Spach; Köse et al., 2013) were used. In the western Mediterranean, in central Spain, higher frequency of exceptionally dry summers has been detected to exist since the beginning of the 20th century using a mixed tree-ring network of *Pinus sylvestris* and *P. nigra* ssp. *salzmannii* covering the past four centuries (Ruiz-Labourdette et al., 2014), whereas a 800-year temperature reconstruction from southeastern Spain using a site of *P. nigra* underlined predominantly higher summer temperatures during the transition between the Medieval Climate Anomaly and the Little Ice Age (Dorado Liñán et al., 2015). A recent reconstruction of spring–late summer temperature from the Pyrenees by means of a *P. uncinata* MXD network dating back to 1186 (Büntgen et al., 2017) underlines warm conditions around 1200 and 1400 and after 1850.

Reconstructions of past droughts and wet periods over the Mediterranean region have been created using climatic indices such as the standardized precipitation index (SPI; McKee et al., 1995) in Spain (modeling 12-month July SPI using several species of the *Pinus* genus; Tejedor et al., 2016), and in Romania (modeling 3-month August standardized SPI using *P. nigra*; Levanič et al., 2013), which allows for the identification of common large-scale synoptic patterns. Droughts have been reconstructed using the Palmer drought severity index (PDSI; Palmer, 1965). Using actual and estimated multispecies tree-ring data, Nicalut et al. (2008) found that the drought episodes at the end of the 20th century are similar to those in the 16th and 17th centuries for the western Mediterranean, whereas in the eastern parts of the region, the droughts seem to be the strongest recorded in the past 500 years.

Early summer temperature has been reconstructed for 400 years in Albania, from a *P. nigra* tree-ring network, finding stable climate–growth relationships over time and a spatial extent of the reconstruction spanning over the Balkans and southern Italy (Levanič et al., 2015). Currently, two summer temperature reconstructions close to the study area and based on maximum latewood density (MXD) chronologies are available: (1) a reconstruction of AS temperatures published by Trouet (2014) covering the period 1675–1980 and centered on the northeastern Mediterranean–Balkan region includes sites from the Italian Peninsula (used in this paper), the Balkan area, Greece and sites from the central and eastern European Alps to central Romania and Bulgaria, the latter areas being characterized by continental climates, and (2) a reconstruction of JAS temperatures published by Klesse et al. (2015), covering the period 1521–2010 and based on a chronology from Mt. Olympus (Greece). As

separate climate (temperature) reconstructions for the north-eastern Mediterranean–Balkan region including Italy have been published to date, the goal of this study was to collect dendrochronological data from Italian research groups and screen the ITRDB for suitable data for climate reconstructions. We therefore investigate RW and MXD climate signals across Italy. After carefully testing the climatic signals recorded in the tree-ring RW and MXD from different sites and different species, the reconstruction that is proposed in this study is the first one including only forest sites from the Italian Peninsula.

Overall, the main objectives of this paper are as follows:

i. To identify the most important climatic drivers modulating tree-ring width (RW) and tree-ring maximum latewood density (MXD) variability in forest sites from central and southern Italy. To our knowledge, this is the first attempt performed in Italy with the clear objective to find common response patterns in conifer and broadleaf species using a multispecies tree-ring network and site-specific historical climatic records.

ii. To estimate the temporal stability of the climate–growth and climate–density relationships.

iii. To perform a climatic reconstruction based only on trees *highly sensitive to climate* (HSTC).

iv. To estimate the spatial coherence of the obtained reconstruction in the region.

2 Data and methods

2.1 Study area and study sites

The study region includes the whole Italian Peninsula and eastern Sicily and covers a latitudinal range from 37 to 44°43′ N (Fig. 1). The peninsula is roughly oriented NW–SE and its longitudinal axis is characterized by the Apennines that reach their maximum altitude at their center (Corno Grande, 2912 m a.s.l., Gran Sasso Massif); a higher altitude is reached in eastern Sicily by the Etna Volcano (3350 m a.s.l.). The study region is surrounded by the Tyrrhenian and Adriatic Seas and is characterized by a typical Mediterranean climate, with high temperatures and low precipitation during the summer (from June to September), and by a Mediterranean-temperate regime at the higher altitudes of the Apennines (Fig. 2). Considering the climatic means at all the study sites (at a mean elevation of 1225 ± 520 m a.s.l.) over the period 1880–2014, the temperatures over the study region range from 0.2 °C (January) to 17.6 °C (in July and in August) and only 11 % of the total annual precipitation falls during the summer (from June to August: 155 mm), whereas 34 % falls during winter (from December$_{-1}$ to February: 493 mm). Autumn is the second wettest season (31 % of total annual precipitation) and spring is the third wettest (24 % of total annual precipitation; Fig. 2).

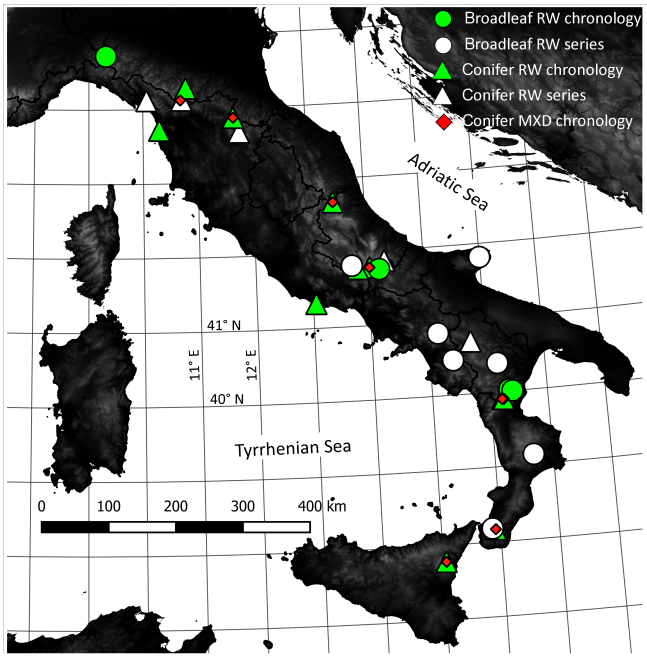

Figure 1. Distribution of the tree-ring sites from central and southern Italy available to the NEXTDATA project and used in this study. Sites were subdivided by the type of tree (conifer or broadleaf), parameter (RW or MXD) and data used (site chronology or only tree-ring series).

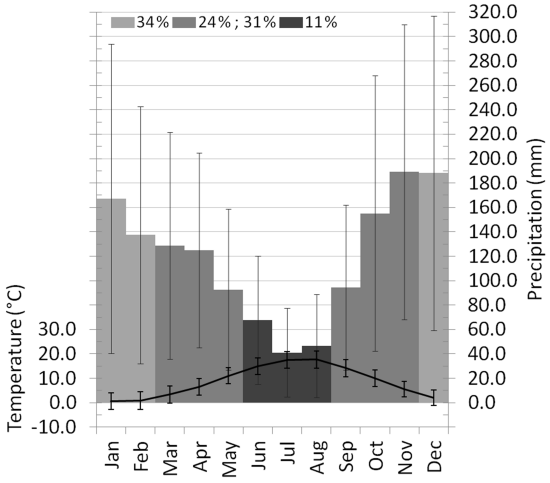

Figure 2. Monthly mean temperatures and precipitation over the period of 1880–2014 for all sites considered in this study. For both temperature and precipitation, the error bars indicate 1 standard deviation; for precipitation, the seasonal percentages of precipitation with respect to the mean annual value (i.e., 1433 mm) are reported.

The total forest cover in Italy, excluding the regions of the European Alps, is approximately 5.8 million hectares (Corpo Forestale dello Stato, 2005), 28 % of the considered surface. Forests characterize the landscape of the inner portion of the Apennine range, at middle to high elevations, and an addi-

tional 1.4 million hectares are covered by woodlands and shrublands, which are the Mediterranean "macchia" that border the forests at low elevations and in areas relatively close to the sea. Overall, broadleaf species are much more abundant in the study region than conifer species, accounting for approximately three-fourths of the forest cover (Dafis, 1997).

The study sites are distributed along the whole latitudinal range of the Italian Peninsula and tree-ring proxies include both RW and MXD series collected within the NEXTDATA project, from Italian universities, and from the ITRDB (www.ncdc.noaa.gov site consulted on September 2015; see Table 1 for full bibliographic references). The data set is based on 27 forest sites composed of several species (conifers at 16 sites, and broadleaves at 11 sites), from which tree-ring series of conifers (RW and MXD) and of broadleaves (RW) were prepared (Fig. 1, Table 1).

2.2 Climate variables

The availability of long and reliable time series of meteorological variables, possibly from stations located very close to forest sites, is crucial for estimating the climate–growth relationships. However, global or regional climatological data sets frequently lack local resolution, especially in remote sites. We, therefore, reconstructed synthetic records of monthly temperature and precipitation series to be representative of the sampled sites using the anomaly method (New et al., 2000; Mitchell and Jones, 2005), as described in Brunetti et al. (2012). Specifically, we reconstructed independently climatological normals following the procedure described in Brunetti et al. (2014) and Crespi et al. (2017) by estimating a local temperature (precipitation)–elevation relationship, and exploiting a very high density data set from time series that are at least 30 years long. We also estimated the deviations from the normals by means of a weighted average of neighboring series, by exploiting the great amount of very long and high quality temperature and precipitation series available for Italy over the past 200–250 years (obtained from an improved version of Brunetti et al., 2006). Finally, by the superposition of the two fields, we obtained temporal series in absolute values for each sampling site. The climate series start in different years due to data availability; however, most of the series start around the mid-19th century. Finally, in order to characterize meteorological drought conditions, we calculated the monthly SPI at timescales of 1, 2, 3, 6, 9 and 12 months for all sites, based on the monthly values of precipitation, using the SPI_SL_6 code of the National Drought Mitigation Center at the University of Nebraska (http://drought.unl.edu).

2.3 Chronology construction, climate sensitivity and climate reconstructions

Raw data. We examined all individual series of RW and MXD for correct dating using visual and statistical cross-dating. In particular, we used statistical techniques to remove potential dating errors by comparing each individual series from one site against the mean site chronology, which was constructed excluding the analyzed individual series. Using the COFECHA software (www.ldeo.columbia.edu), the individual series were moved forward and backward 10 years from their initial positions, and similarity indices were calculated over a 50-year time window, thus highlighting the potential dating errors.

Site chronologies. We used the regional curve standardization approach (RCS; Briffa et al., 1992; Briffa and Melvin, 2011; Esper et al., 2003) both with the RW and MXD series to preserve the low-frequency variability in the site chronologies. We used the ARSTAN software (ver. 44 h3, www.ldeo.columbia.edu) and did not consider the pith offset estimates between the first measured ring and the actual first year of growth (Esper et al., 2009; Leonelli et al., 2016). The regional curve (RC) for the mean chronology, which was obtained after the series alignment to the first measured ring, was smoothed using a cubic spline with a width of 10 % of the chronology length (Büntgen et al., 2006). We computed ratios of raw measurements vs. the values of growth predicted by the RC for all years of the individual series, and the resulting indexed series were averaged by a biweight robust mean to obtain the site chronologies of RW and of MXD. We constructed the RW and MXD site chronologies only for sites with at least 10 individual series fulfilling the following conditions: (i) the individual series length was >100 years; (ii) the individual series correlation with the respective site chronology had $r>0.3$; (iii) the mean inter-series correlation (MIC) had $r>0.3$; and (iv) the expressed population signal (EPS; Wigley et al., 1984; Briffa and Jones, 1990) was >0.7. We used only the individual series fulfilling these conditions to construct the site chronologies. However, we accepted some exceptions in order to maximize the number of sites and chronologies available for analysis (see exceptions in Table 1).

Climate sensitivity. We assessed species-specific climate sensitivity for the constructed RW and MXD site chronologies over the common period of 1880–1980 using correlation analysis and the site-specific monthly variables of temperature, precipitation and standardized precipitation index, from March of the year prior to growth to September of the year of growth. We computed correlations using the DENDROCLIM software (Biondi and Waikul, 2004), applying a bootstrap with 1000 iterations, and the obtained results were analyzed by grouping together conifer and broadleaf species.

Testing for climate–growth relationships at the site level. To assess the influence of environmental settings on climate–growth relationships, for the conifer MXD site chronolo-

Table 1. References for all the dendrochronological data used in this research, information on site locations, types of parameter used at each site and the tree species. Sites are ordered along a decreasing latitudinal gradient, after differentiating between conifers and broadleaves (horizontal line).

Database information and site location								Type of tree-ring parameter			
Data set name	Database source	Original contributor	Bibliographic reference	Location name	Latitude N	Longitude E	Elevation (m a.s.l.)	RW chr.	RW series	MXD chr.	Species
ITRDBITAL017	ITRDB	Ori (2015)	https://www.ncdc.noaa.gov/paleo/study/4079	Monte Cantiere	44°16′48″	10°48′00″	800	x			*Pinus* sp.
ITRDBITAL009	ITRDB	Schweingruber (2015a)	https://www.ncdc.noaa.gov/paleo/study/4301	Abetone	44°07′12″	10°42′00″	1400		x	x	*Abies alba*
ITRDBITAL004	ITRDB	Biondi (2015b)	https://www.ncdc.noaa.gov/paleo/study/2753	Campolino	44°06′45″	10°39′44″	1650		x		*Picea abies*
ITRDBITAL008	ITRDB	Schweingruber (2015f)	https://www.ncdc.noaa.gov/paleo/study/4540	Mount Falterona	43°52′12″	11°40′12″	1450	x		x	*Abies alba*
ITRDBITAL003	ITRDB	Biondi (2015d)	https://www.ncdc.noaa.gov/paleo/study/2760	Pineta San Rossore	43°43′12″	10°18′00″	5	x			*Pinus pinea*
ITRDBITAL022	ITRDB	Becker (2015)	https://www.ncdc.noaa.gov/paleo/study/2706	Pratomagno Bibbiena – Appennini	43°40′12″	11°46′12″	1050		x		*Abies* sp.
ITRDBITAL012	ITRDB	Schweingruber (2015c)	https://www.ncdc.noaa.gov/paleo/study/4374	Ceppo Bosque di Martense	42°40′48″	13°25′48″	1700	x		x	*Abies alba*
Abies-Abeti-Soprani	UNIMOL			Colle Canalicchio-Abeti Soprani	41°51′40″	14°17′51″	1350		x		*Abies alba*
ITRDBITAL016	ITRDB	Schweingruber (2015e)	https://www.ncdc.noaa.gov/paleo/study/4536	Monte Mattone	41°46′48″	14°01′48″	1550	x		x	*Pinus nigra*
ITRDBITAL001	ITRDB	Biondi (2015a)	https://www.ncdc.noaa.gov/paleo/study/2752	Camosciara Mt. Amaro	41°46′12″	13°49′12″	1550	x			*Pinus nigra*
ITRDBITAL002	ITRDB	Biondi (2015c)	https://www.ncdc.noaa.gov/paleo/study/2759	Parco del Circeo	41°19′48″	13°03′02″	5	x			*Pinus pinea*
AAIBA	UNIBAS			Ruoti (PZ)	40°42′04″	15°43′43″	925		x		*Abies alba*
ITRDBITAL011	ITRDB	Schweingruber (2015g)	https://www.ncdc.noaa.gov/paleo/study/4541	Mount Pollino	39°54′00″	16°12′00″	1720	x		x	*Abies alba*
ITRDBITAL015	ITRDB	Schweingruber (2015h)	https://www.ncdc.noaa.gov/paleo/study/4644	Sierra de Crispo	39°54′00″	16°13′48″	2000	x		x	*Pinus leucodermis*
ITRDBITAL010	ITRDB	Schweingruber (2015d)	https://www.ncdc.noaa.gov/paleo/study/4420	Gambarie Aspromonte	38°10′12″	15°55′12″	1850	x		x	*Abies alba*
ITRDBITAL013	ITRDB	Schweingruber (2015b)	https://www.ncdc.noaa.gov/paleo/study/4304	Etna Linguaglossa	37°46′48″	15°03′00″	1800	x		x	*Pinus nigra*
ITRDBITAL019	ITRDB	Nola (2015)	https://www.ncdc.noaa.gov/paleo/study/4042	Corte Brugnatella	44°43′12″	09°19′12″	900	x			*Quercus robur*
Fagus-Parco-Abruzzo	UNIMOL			Val Cervara	41°49′00″	13°43′00″	1780		x		*Fagus sylvatica*
Fagus-Gargano	UNIMOL			Parco Nazionale del Gargano Riserva Pavari	41°49′00″	16°00′00″	775		x		*Fagus sylvatica*
Fagus-Montedimezzo	UNIMOL			Riseva MaB Unesco Collemeluccio-Montedimezzo	41°45′00″	14°12′00″	1100	x			*Fagus sylvatica*
Cervialto-FASY	UNINA2			Monti Picentini	40°50′23″	15°10′03″	800		x		*Fagus sylvatica*
Fagus-Cilento	UNIMOL			Parco Nazionale del Cilento Ottati	40°28′00″	15°24′00″	1130		x		*Fagus sylvatica*
QCIBG	UNIBAS			Gorgoglione (MT)	40°23′09″	16°10′04″	820		x		*Quercus cerris*
QFIMP1	UNIBAS			San Paolo Albanese (PZ)	40°01′20″	16°20′26″	1050	x			*Quercus frainetto*
QFIMP2	UNIBAS			Oriolo (CS)	40°00′10″	16°23′29″	960	x			*Quercus frainetto*
Fagus-Sila	UNIMOL			Parco Sila	39°08′00″	16°40′00″	1680		x		*Fagus sylvatica*
Fagus-Parco-Aspromonte	UNIMOL			Aspromonte	38°11′00″	15°52′00″	1560		x		*Fagus sylvatica*
							1235 mean elevation	15 sites	12 sites	8 sites	

gies (i.e., the chronologies holding the strongest climatic signal; see Results), we performed a redundancy analysis (RDA) selecting the bootstrapped correlation coefficients of climate–growth relationships (Fig. 3) as response variables and the environmental variables as explanatory variables (geographical characteristics and climatic averages over the period 1880–1980). In order to attenuate co-variation within the environmental variables, we ran a principal component analysis (PCA) before the RDA and the following variables were finally chosen: elevation (co-varying with longitude: our sites are placed at higher elevation at increasing longitude; Table 1); average AS temperature; average JJA precipitation (co-varying with latitude: higher latitude means higher precipitation amounts); average JJAS SPI_3 (at timescale of 3 months, i.e., the timescale resulting most significant; see Results). Moreover, for each of the MXD site chronologies, we calculated the site fitness (SF; Leonelli et al., 2016), representative of the percentage of selected HSTC series of conifer MXD with respect to the total of series available at each site.

We used the results of the climate sensitivity analysis to detect the *driving climate variables* (DCVs; of temperature, precipitation and SPI) for each of the three groups of chronologies: MXD conifer, RW conifer and RW broadleaf. Specifically, for each group of chronologies and for each climate variable, we first identified the months with significant correlations at most sites (> 50 %) and with mean correlation values of $|\overline{r}| > 0.25$ (black-filled squares in Fig. 3). Starting from the monthly climatic averages of the sites presenting significant correlations with these selected months, we constructed regional climate series by z scoring the monthly series of each site and calculating regional mean departures; the series of each site were then completed over the maximum period covered by data and reconverted in original units (based on regional mean departures and their specific means and standard deviations), and finally averaged between sites. We calculated the DCVs as means of 2–4 consecutive months of the regional series, except for August$_{-1}$ temperature vs. conifer RW (according to what was obtained in the site-level analysis of Fig. 3).

HSTC chronologies. Based on the available RW and MXD indexed individual series from all of the sites, we constructed six HSTC chronologies, as in Leonelli et al. (2016). However, given the smaller number of data sets available in this study and the shortness of the time series, a modified version of the method was applied. Specifically, we tested all of the RW (conifer and broadleaf) and MXD (only conifer) indexed individual series against each of the above-defined six DCVs, and we used only the individual tree-ring indexed series with correlation values of $|\overline{r}| > 0.25$ in both of the 100-year subperiods of the climatic data set (1781–1880 and 1881–1980) for building each of the six HSTC chronologies (which was done by simply averaging together the selected indexed series). We constructed the six HSTC chronologies starting from all of the indexed individual series of conifer MXD (148 series), of conifer RW (245) and of broadleaf RW (140), which were previously obtained, while constructing the site chronologies (indexed individual series from sites not meeting the fixed quality standards for a site chronology were included at the beginning of the selection).

Climate sensitivity through time. To test the stability of the climate signals recorded in the HSTC chronologies, we conducted a moving correlation analysis between the six HSTC chronologies and their respective DCV, computing bootstrapped correlation coefficients with DENDROCLIM over 60-year time windows that were moved 1 year per iteration over the longest available periods.

Climate reconstruction. We used only the HSTC chronology showing the highest absolute values of correlation and the most stable signal over time (i.e., the conifer MXD for late summer temperature; see Results) for the climate reconstruction. To extend this HSTC chronology as far back in time as possible, we also added the oldest available individual MXD indexed series with correlations of $|\overline{r}| > 0.25$ with this chronology and which had a minimum length of 100 years. For constructing the chronology for climate reconstruction, we applied an arithmetic mean to the indexed series, after having normalized all individual series over the common period 1879–1962. Moreover, to account for the changing sample size through time, a variance stabilization of the resulting chronology was performed using Briffa's RBAR-weighted method (Osborn et al., 1997). In order to improve the HSTC chronology over the early period showing an EPS $< \sim 0.8$ (i.e., before 1713 in the first version of the HSTC chronology), we considered the yearly difference of the indexed normalized series from the mean and discarded the early portion of the series exceeding the threshold of 2.5 standard deviations in a given year (one series was truncated at 1713, whereas the other nine fell within a common variability). Finally, we re-normalized all series and recalculated the final version of the HSTC chronology used for the temperature reconstruction as described above. We calibrated and verified linear regression and scaling models (Esper et al., 2005) over the 100-year periods 1781–1880 and 1881–1980, respectively, and then the same was done over the inverted periods, in order to estimate model performances and stability. We computed reduction of error (RE; Fritts, 1976) and coefficient of efficiency (CE; Briffa et al., 1988) statistics to assess the quality of the reconstructions. We then used the reconstructed series of late summer temperatures over the period 1901–1980 to build a spatial correlation map with the KNMI Climate Explorer (https://climexp.knmi.nl/; Trouet and van Oldenborgh, 2013), using the 0.5° grid of August–September average temperature and of AS average precipitation (CRU TS 4.0, Climatic Research Unit, University of East Anglia Harris et al., 2014). We used this independent data set instead of the Italian one, as our primary goal was to analyze how far from the Italian Peninsula the reconstructed climatology is still representative.

Table 2. Main characteristics of the chronologies used in this research, separating RW (comprised of both broadleaf and conifer species) and MXD (only conifer species). For each site and parameter, the total number of series available and the number of series showing a correlation value $0.2 < r < 0.3$ with the respective master chronology is reported. Values in bold are those that do not exceed the fixed thresholds of MIC > 0.3, EPS > 0.7 and a number of series > 10, determining the exclusion of the chronology from further analyses. Sites ordered as in Table 1.

	RW series characteristics							MXD series characteristics on the maximum period available						
Data set name	Start date	End date	Time span	MIC[a]	EPS[b]	no. series	no. series $0.2 < r < 0.3$ vs. master	Start date	End date	Time span	MIC1	EPS2	no. series	no. series $0.2 < r$
ITRDBITAL017	1856	1989	134	0.43	0.76	14	0	–	–	–	–	–	–	–
ITRDBITAL009	[1846]	[1980]	[135]	[0.73]	[**0.66**]	13	0	1846	1980	135	0.76	0.86	21	0
ITRDBITAL004	[1836]	[1988]	[153]	[0.51]	[**0.49**]	11	0	–	–	–	–	–	–	–
ITRDBITAL008	1827	1980	154	0.62	0.70	12	0	1827	1980	154	0.66	0.87	12	0
ITRDBITAL003[1]; [2]	1861	1988	128	0.51	0.72	**9**	0	–	–	–	–	–	–	–
ITRDBITAL022[3]	[1539]	[1972]	[434]	[0.45]	[**0.67**]	**6**	1	–	–	–	–	–	–	–
ITRDBITAL012	1654	1980	327	0.57	0.85	26	0	1654	1980	327	0.59	0.91	25	0
Abies-Abeti-Soprani[1]	[1838]	[2005]	[168]	[0.53]	[**0.50**]	11	0	–	–	–	–	–	–	–
ITRDBITAL016	1844	1980	137	0.54	0.84	17	0	1844	1980	137	0.43	0.75	15	0
ITRDBITAL001	1750	1987	238	0.52	0.77	16	0	–	–	–	–	–	–	–
ITRDBITAL002[1]	1878	1988	111	0.51	0.72	16	0	–	–	–	–	–	–	–
AAIBA[1]	[1866]	[2007]	[142]	[0.51]	[**0.55**]	13	0	–	–	–	–	–	–	–
ITRDBITAL011	1800	1980	181	0.58	0.85	20	0	1800	1980	181	0.54	0.84	18	0
ITRDBITAL015	1415	1980	566	0.58	0.95	22	0	1441	1980	540	0.50	0.76	21	0
ITRDBITAL010	1790	1980	191	0.53	0.76	19	0	1790	1980	191	0.50	0.85	18	0
ITRDBITAL013	1773	1980	208	0.57	0.88	20	0	1795	1980	186	0.44	0.78	18	0
ITRDBITAL019	1779	1989	211	0.54	0.82	16	0	–	–	–	–	–	–	–
Fagus-Parco-Abruzzo	[1716]	[2008]	[293]	[0.36]	[0.73]	**3**	0	–	–	–	–	–	–	–
Fagus-Gargano	[1821]	[2009]	[189]	[**0.23**]	[**0.42**]	**3**	3	–	–	–	–	–	–	–
Fagus-Montedimezzo	1844	2005	162	0.67	0.85	15	0	–	–	–	–	–	–	–
Cervialto-FASY	[1828]	[2003]	[176]	[0.39]	[**0.52**]	10	0	–	–	–	–	–	–	–
Fagus-Cilento	[1837]	[2007]	[171]	[0.41]	[**0.26**]	**7**	1	–	–	–	–	–	–	–
QCIBG[1]; [3]	[1897]	[2013]	[117]	[0.60]	[**0.66**]	**9**	0	–	–	–	–	–	–	–
QFIMP1	1851	2013	163	0.50	0.78	34	0	–	–	–	–	–	–	–
QFIMP2	1854	2013	160	0.55	0.79	34	0	–	–	–	–	–	–	–
Fagus-Sila	[1854]	[2009]	[156]	[0.30]	[**0.21**]	**4**	3	–	–	–	–	–	–	–
Fagus-Parco-Aspromonte	[1874]	[2009]	[136]	[**0.27**]	[-**0.42**]	**5**	2	–	–	–	–	–	–	–
TOTAL	1785[4]	1989[4]	205[4]	0.55[4]	0.80[4]	385	10	1750	1980	231	0.55	0.83	148	0
	mean	mean	mean	mean r	mean EPS	sum (all sites)	sum (all sites)	mean	mean	mean	mean r	mean EPS	sum	sum (all sites)

[a] Mean inter-series correlation of raw series, calculated using the maximum period available at each site. [b] Expressed population signal of indexed series in the common period of 1880–1980. [1] Series up to 80 years included.
[2] Chronology built with fewer than 10 series (good EPS). [3] Common period with later start date or earlier end date. [4] Sites without chronology [....] are not included in the computation.

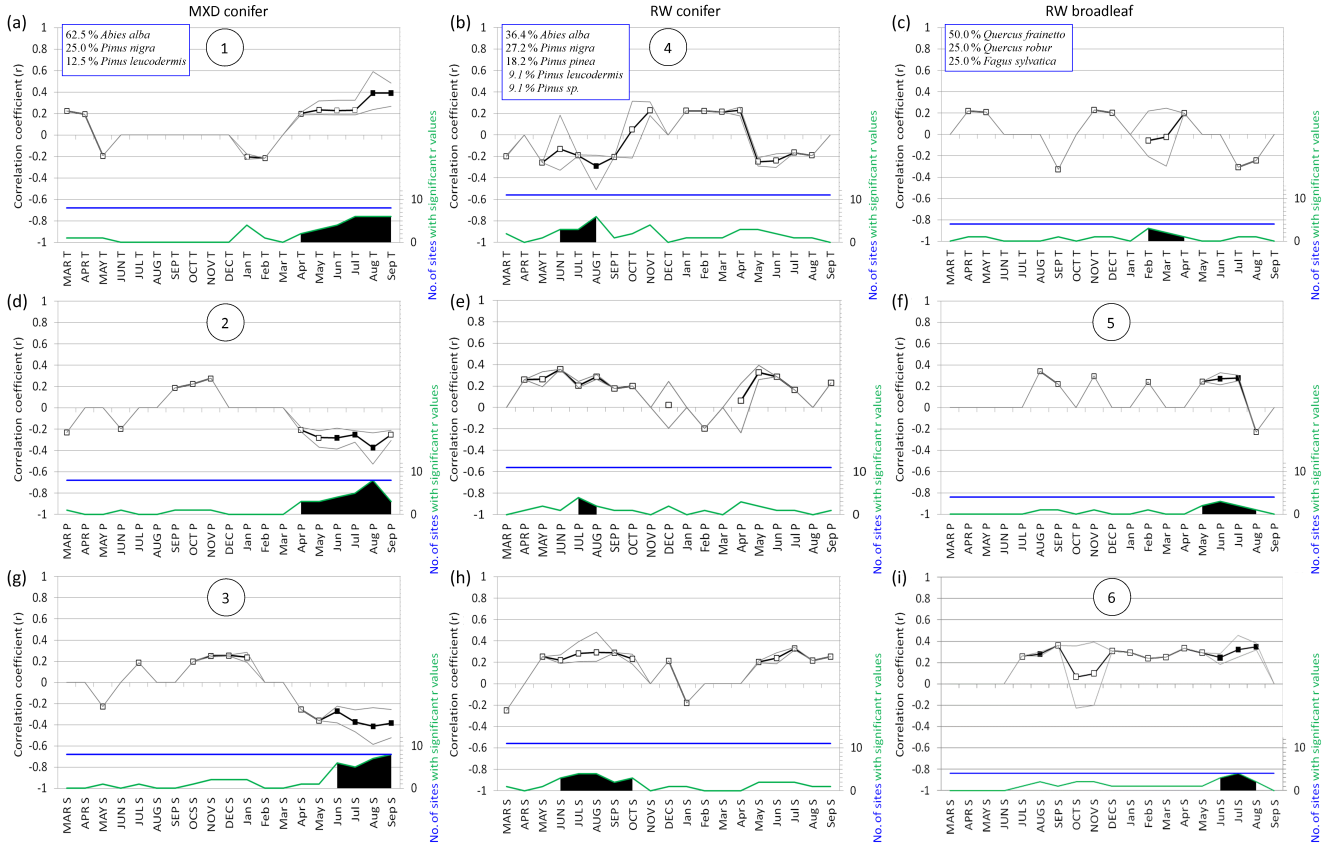

Figure 3. Bootstrapped correlation analysis performed over the common period of 1880–1980, considering chronologies of conifer MXD (left column; **a, d, g**), of conifer RW (center; **b, e, h**) and of broadleaf RW (right; **c, f, i**) vs. monthly temperature **(a, b, c)**, precipitation **(d, e, f)** and SPI_3 **(g, h, i)** from March of the year prior to growth to September of the year of growth. In **(a)**, **(b)**, **(c)** the percentages of the species composing the pool for each site used for the analysis is reported. Means of statistically significant ($p < 0.05$) correlation coefficient values (r) are depicted with squares, whereas maximum and minimum significant r values are indicated with grey lines; the blue lines depict the total number of sites in each comparison and the green lines indicate the total number of sites with statistically significant r values. Black-filled squares are given for those variables that show significant correlation values for at least 50 % of the total sites and have $|\bar{r}| > 0.25$; where both conditions occur, a circled number in the plot is given and the comparisons are selected for the following moving correlation analysis (Fig. 5). In each plot the climate variables with the highest number of sites with significant r values and nearby variables showing up to one-half of this number are depicted with a black area.

3 Results

Site chronologies. We obtained 15 RW site chronologies (11 from conifers and 4 from broadleaves) and 8 MXD site chronologies (from conifers) and we used them to estimate climate sensitivity at the site level and to detect the most important climatic drivers over the study region (for species percentages, see boxes in Fig. 3a, b and c). We performed the construction of the HSTC chronologies (for the analysis of the temporal stability of climate signals and for climate reconstruction) using also the individual series from the 12 sites (5 from conifers and 7 from broadleaves; see Table 1, bold values in Table 2 and Sect. 2) for which the site chronologies did not meet the quality standards. The maximum time span of tree-ring data covers the period from 1415 (ITRDBITAL015) to 2013 (QFIMP1 and QFIMP2). However, the mean chronology length is 215 ± 130 years for conifers and 175 ± 25 years for broadleaves (values rounded to the nearest 5 years; Table 2). Over the common period considered (1880–1980 for all MXD and RW chronologies), the mean series intercorrelation and expressed population signal are approximately 0.5 and 0.8, respectively.

Tree-ring sensitivity to climate. The site-specific sensitivity analysis performed over the common period of 1880–1980 revealed that MXD in conifers records stronger climatic signals than RW in either conifers or broadleaves, in terms of the average correlation coefficient, the number of months showing statistically significant values ($p < 0.05$) and the fraction of chronologies (over the maximum number available) responding to the same climatic variable (Fig. 3). In particular, all conifer MXD chronologies were found to be positively influenced by late summer temperatures (Au-

gust and September), whereas precipitation from June to August is negatively correlated with most of them (Fig. 3a and b). In terms of SPI, the highest correlations (for both MXD and RW) were obtained for the indices calculated at the timescales of 2 and 3 months (only the SPI at 3 months, SPI_3, is reported in the Results), while longer timescales showed fewer significant correlation values. Most conifer MXD were found to be negatively correlated with SPI_3 from June to September, highlighting that low index values, i.e., drought periods, are associated with high MXD in the tree rings, and vice versa (Fig. 3c).

For conifer RW, significant correlation coefficients, i.e., those exceeding the mean value of $|\bar{r}| > 0.25$ for more than 50 % of the available chronologies, were obtained only for the August temperatures of the year prior to growth (a negative correlation; Fig. 3b). In the other months, correlations are generally low and sometimes show opposite signs for the same climatic variable. However, a slightly stronger influence from the climatic variables for the summer months prior to growth can be noted (black areas in Fig. 3a, d and g).

Broadleaf RW were found to be positively influenced by high precipitation and low drought occurrences (high SPI_3 values) during the summer months (June and July precipitation and June to August SPI_3; Fig. 3f and i), whereas the temperature did not show a significant influence (Fig. 3c).

Influence of environmental settings on climate–growth relationships and site fitness. We found that the strength of the AS signal correlated positively with latitude (mean precipitation) and negatively with elevation (longitude; Fig. 4a). Summer precipitation amounts and elevation correlated negatively in our data set of MXD, revealing the dominance of the latitudinal gradient of larger precipitation in northern areas over the expected altitudinal gradient of higher precipitation at higher altitudes: sites in northern areas, even if at lower altitudes, receive more summer precipitation than sites in southern regions at higher altitude. The RDA analysis revealed that both parameters were on opposing sides of the first two axes explaining 89.55 % of the variance of the data set: the F1 axis alone explains up to 72 % of the variance in response variables, and especially in AS temperature and JJAS SPI_3 signals. Concerning site fitness, especially sites located at higher latitudes, in particular north of 42° N (all of *Abies alba*) presented values of SF > 80 %, and up to 86 % (Fig. 4b). South of 42° N, all sites (including two sites of *Abies alba*) presented an SF of approximately 10 %, with the *Pinus leucodermis* site showing the highest SF value (52 %) and a *P. nigra* site the lowest (0 %).

Stability of the climatic signal over time. The six comparisons performed between the HSTC chronologies and the DCVs were deemed important to understand the influence of temporal climatic variability on conifers MXD and RW and on broadleaf RW (Fig. 5). The moving-window correlation analysis revealed that the HSTC conifer MXD chronology held the strongest and most stable climatic signal of late summer temperature over time, with values of correlation co-

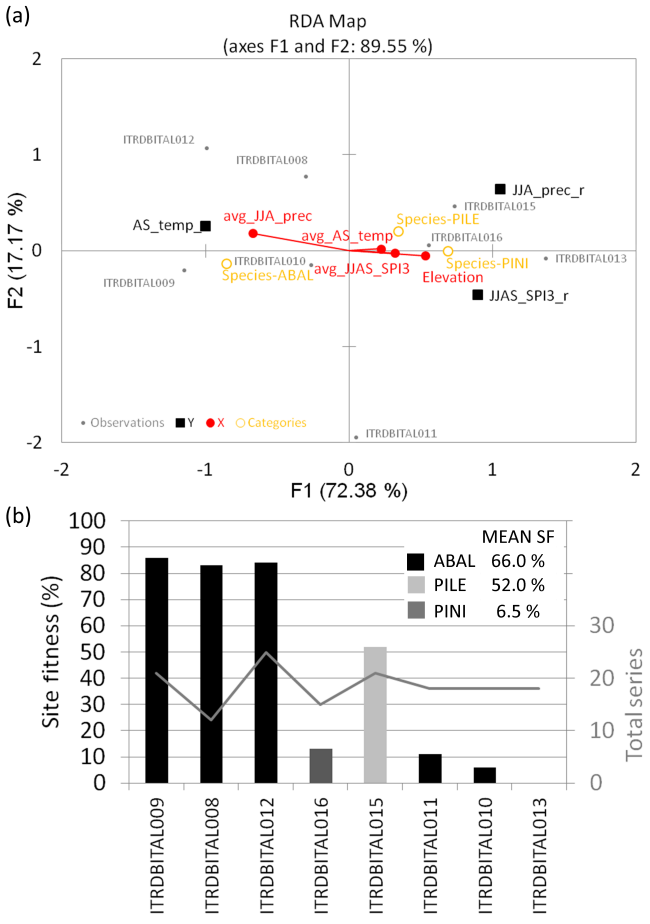

Figure 4. Ordination biplot (RDA analysis) of climate–growth relationships (response variables, Y) and environmental settings (explanatory variables X: elevation and climatic averages over the period 1880–1980) **(a)**. Site fitness evaluated on single indexed series included in the MXD HSTC chronology (SF; Leonelli et al., 2016) and total series per site (grey line) **(b)**. Sites are ordered with decreasing latitude along the x axis. Mean SF values for each species are also reported. ABAL stands for *Abies alba*; PILE stands for *Pinus leucodermis*; PINI stands for *Pinus nigra*.

efficient ranging from approximately 0.4 to nearly 0.8 in the more recent periods analyzed (curve 1 in Fig. 5). In the other two HSTC chronologies based on conifer MXD (curve 2 and 3 in Fig. 5), starting from the time window 1881–1940 up to recent periods, we always found higher absolute values for SPI_3 than for precipitation, with values of correlation reaching approximately −0.7 and −0.6, respectively, (curve 3 and 2 in Fig. 5). For the conifer RW, a strong change in the temperature signal of August prior to growth was found (curve 4 in Fig. 5), with correlation values shifting from positive (and statistically non-significant) in the early period of analysis to negative (approximately −0.5) in the middle to late analysis period. The two HSTC chronologies of broadleaf RW showed nearly the same correlation values and similar patterns with both the June and July precipitation and the June